EXPOSING IMAGE FORGERY THROUGH THE DETECTION OF CONTRAST ENHANCEMENT

Xufeng Lin, Chang-Tsun Li and Yongjian Hu

Department of Computer Science, University of Warwick, Coventry CV4 7AL, UK

ABSTRACT

In this paper, a novel forensic method of exposing cut-and-paste image forgery through detecting contrast enhancement is proposed. We reveal the inter-channel correlation introduced by color image interpolation, and show how a linear or nonlinear contrast enhancement can disturb this natural inter-channel dependency. We then construct a metric to measure these correlations, which are useful in distinguishing the original and contrast enhanced images. The effectiveness of the proposed algorithm is experimentally validated on natural color images captured by commercial cameras. Finally, its robustness against some anti-forensics algorithms is also discussed.

Index Terms— Digital forensics, contrast enhancement, demosaicking, inter-channel correlation

1. INTRODUCTION

In a typical cut-and-paste image forgery scene, the background of pasted region is not usually consistent with that of duplicated region, so contrast enhancement is widely used to avoid leaving obvious visual clues. However, a number of contrast enhancement operations are equivalent to pixel value mappings, which will introduce some statistical traces. Therefore, we can expose cut-and-paste image forgery by detecting contrast enhancement. A blind method is proposed in [1] to detect globally and locally applied contrast enhancement operations, which introduce sudden peaks and zeros in the histogram and therefore increase high-frequency components in the histogram spectrum. It achieves good results by comparing the high-frequency measurement of histogram spectrum with a threshold. But it is not convenient to use in practice as there are some parameters to be determined. What's more, some corresponding anti-forensics algorithms have been put forward. In this work, we propose a novel contrast enhancement detection approach using inter-channel similarities of high-frequency components. In comparison with the algorithm described in [1], the performance of algorithm is presented based on experimental results under both forensics and anti-forensics scenarios.

The remainder of this paper is organized as follows: Section 2 briefly reviews the method in [1], then Section 3 describes the proposed detection scheme in details. Experimental results and the conclusions are provided in Section 4 and Section 5, respectively.

2. HISTOGRAM-BASED DETECTION OF CONTRAST ENHANCEMENT

Due to observational noise [2], sampling effects, complex lighting environments and CFA interpolation, the image histograms do not contain sudden zeros or impulsive peaks, so that an unaltered image's histogram is strongly low pass. While contrast enhancement manipulation will expand or squeeze the original histogram and lead to sudden peaks and gaps in the histogram, which causes the increase of high-frequency energy in the histogram spectrum. Based on this observation, [1] propose a general contrast enhancement detection algorithm:

(1) Obtain the image's histogram $h(x)$ and calculate the modified histogram $g(x)$ as follows,

$$g(x) = h(x)p(x) \tag{1}$$

where $p(x)$ is a pinch off function, whose role is to eliminate low end or high end saturated effect in images.

(2) Transform $g(x)$ into discrete Fourier frequency domain, $G(k)$, and calculate the high-frequency measurement F according to

$$F = \frac{1}{N}\sum_{k} |\beta(k)G(k)|, k = 0, 1, ..., 255 \tag{2}$$

where N is the total number of pixels, and $\beta(k)$ is the cutoff function deemphasizing the low frequency components of $G(k)$:

$$\beta(k) = \begin{cases} 1, T \leq k \leq 255 - T \\ 0, \text{else} \end{cases} \tag{3}$$

where T corresponds to a desired cutoff frequency.

(3) Finally, F is compared with a threshold τ to determine whether contrast enhancement has been applied.

Local contrast enhancement can be detected through applying above procedures block by block. But there are some parameters need to be determined by users, such as the pinch off function and the cutoff frequency T. It is not convenient in practice as the optimal parameters may vary with different forms of contrast enhancements. Most important, as the histogram of image can be easily tampered, these kind of histogram-based forensics methods will fail if the traces left on the image histogram have been concealed by attackers. For example, G. Cao et al. remove the peak and gap artifacts of histogram introduced by contrast enhancement using local random dithering [3], which essentially adds Gaussian noise with appropriate variance onto the contrast enhanced image. In [4], M. Barni et al. also propose a universal anti-forensics technique against histogram-based contrast enhancement detector. The histogram h_y of an enhanced image is modified according to the most similar histogram h_x from a reference histogram database while keeping the image distortion as low as possible. In light of this, it is necessary to develop new contrast enhancement detection schemes.

3. PROPOSED ALGORITHM

3.1. Motivation

In the imaging process of most digital cameras, a color filter array (CFA) is placed before the sensor to capture one of the primary colors for each pixel while the other color components are interpolated

with a specific demosaicking algorithm. As human eyes are more sensitive to the green components of visible light, most CFAs tend to sample the G channel at a higher rate than R and B channels. In the well-known Bayer CFA sampling pattern, G samples are twice as many as R and B samples. The spectrum of G channel therefore has less aliasing and its high-frequency components are better preserved. Hence, most of the color interpolation algorithms [5, 6] will replace the high-frequency components of R and B channels with those of G channel, which can be represented by

$$R_h \approx G_h \approx B_h \tag{4}$$

where R_h, G_h and B_h denote the high-frequency bands of interpolated color plane R, G and B. Equation (4) can be interpreted as that R and B "copies" the high-frequency components of G [7]. However, this inter-channel similarity may be altered by some image manipulations, one of which is contrast enhancement. The reasons will be investigated in the following sub-section.

3.2. Proposed algorithm

In this sub-section, we will first show how the contrast enhancement can disturb the inter-channel similarities of high-frequency components, and then propose our detection scheme.

To explore what will happen to the high-frequency components of an image if it is enhanced, we draw the 3D scatter plots of the high-frequency wavelet coefficients of an original image and the corresponding enhanced image in Fig. 1(a) and 1(b). The coordinates of each point denote the values of R, G, and B wavelet coefficients in the diagonal subband, taken at the same pixel location. In general, the points are compactly clustered along the vector $(1, 1, 1)$ for original image, which implies the strong correlation and approximate equality of the wavelet coefficients [8]. For enhanced image, however, the points deviate from the line suggesting the inter-channel correlation has been altered. Next, the reasons for why a linear or nonlinear contrast enhancement can disturb the inter-channel similarity will be explored:

(1) Linear contrast enhancement

Consider an 8-bit image as a signal $x(n)$, and $0 \le x(n) \le 255$. After applying discrete wavelet transformation (DWT) to $x(n)$, the wavelet coefficients at level $j+1$ can be written as [9]:

$$d^{j+1}(k) = \sum_{m=0}^{p-1} h(m) x^j(2k-m) \tag{5}$$

where $h(m)$ is the coefficients of a filter, depending on the chosen wavelet function, and p is the length of $h(m)$. $x^j(n)$ is the approximation coefficients at level j, and $x^0(n) = x(n)$. If $x^j(n)$ is multiplied by a linear scaling factor w, then $x^j(n)$ can be divided into two sets:

$$\begin{cases} X_1 = \{x^j(n) | w * x^j(n) \le 255\} \\ X_2 = \{x^j(n) | w * x^j(n) > 255\} \end{cases} \tag{6}$$

Then the wavelet coefficients become:

$$\begin{aligned} \widetilde{d}^{j+1}(k) = w \sum_{x^j \in X_1} h(m) x^j(2k-m) \\ + w \sum_{x^j \in X_2} h(m) x^j(2k-m) \end{aligned} \tag{7}$$

If $w \le 1$, then $X_2 = \varnothing$, and $\widetilde{d}^{j+1}(k) = w * d^{j+1}(k)$, which means all coefficients are multiplied by the same factor. Therefore, the inter-channel similarity still holds if we separately enhance R, G and B channel. However, it rarely happens in the cut-and-paste forgery scenario as it will result in chromatic aberration. The most common situation is that the RGB image is converted into YUV color space, and contrast enhancement will be only applied in Y channel. In this case, the inter-channel similarity will be disturbed by the mapping from YUV back to RGB. And if $w > 1$, then $X_2 \neq \varnothing$, and all data in X_2 will be truncated to 255, so the approximate equality of high-frequency components will be disturbed in this case.

(2) Nonlinear contrast enhancement

As a signal can be decomposed into cosine waves, for the sake of simplicity, we take a simple 1D signal composed of a sum of two zero-phase cosinusoids for example:

$$x(n) = a\cos(\omega_1 n) + b\cos(\omega_2 n) \tag{8}$$

Then we rewrite nonlinear transformation function $T(x)$ in terms of its Taylor series expansion:

$$\begin{aligned} T(x) &= T(x_0) + T'(x_0)(x-x_0) + \frac{T''(x_0)(x-x_0)^2}{2} \\ &+ \sum_{i=3}^{\infty} \frac{T^{(i)}(x_0)(x-x_0)^i}{i!} \end{aligned} \tag{9}$$

Only considering the first three terms of the right side of Equation (9), it contains x^2, which means after $T(x(n))$ performed, we will have a $x^2(n)$ term:

$$\begin{aligned} x^2(n) &= \frac{a^2}{2}\cos(2\omega_1 n) + \frac{b^2}{2}\cos(2\omega_2 n) \\ &+ ab\cos((\omega_1-\omega_2)n) + \frac{a^2+b^2}{2} \\ &+ ab\cos((\omega_1+\omega_2)n) \end{aligned} \tag{10}$$

Notice the presence of new frequencies $2\omega_1$, $2\omega_2$, $\omega_1 - \omega_2$ and $\omega_1 + \omega_2$ will certainly disturb the similarity of inter-channel high-frequency components.

Based on the above analysis, we construct a metric S to measure the similarity. If the 2D wavelet coefficients of color channel c in the diagonal subband at level i is denoted by $D_c^i(m,n)$, the measurement of inter-channel similarity of high-frequency components can be defined as:

$$S = \frac{1}{MN} \sum_{m=0}^{M-1} \sum_{n=0}^{N-1} \left| D_{c_1}^1(m,n) - D_{c_2}^1(m,n) \right| \tag{11}$$

where $c_1, c_2 \in \{R, G, B\}, c_1 \neq c_2$. M and N is the width and height of the diagonal subband. After S has been calculated, a decision rule is conducted to determine if contrast enhancement has been performed, with values of S greater than the threshold η signifying the detection of contrast enhancement. Similar with [1], we applied block-wise detection for local contrast enhancement. Conceivably, the S of unaltered images is closer to zero than that of altered images. S extracted from linear and nonlinear contrast enhanced images are shown in Fig. 2(a)-(d), which conform with our analysis above. In Fig. 2(b) and 2(c), it is straightforward to show that aside from exceptional cases, the original and enhanced images can be distinguished clearly. And in Fig. (d), taking histogram equalization as a nonlinear contrast enhancement example, all the unaltered and altered images can be classified perfectly using the proposed detection scheme.

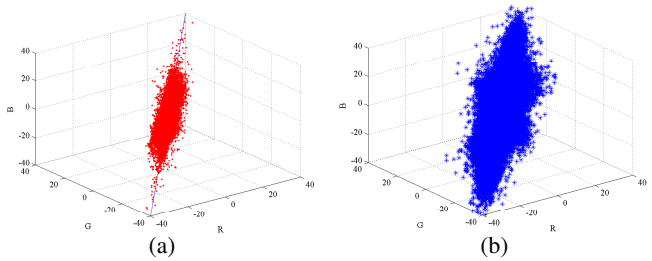

(a) (b)

Fig. 1. Scatter plots of wavelet coefficients in diagonal subband for (a) original image and (b) enhanced image.

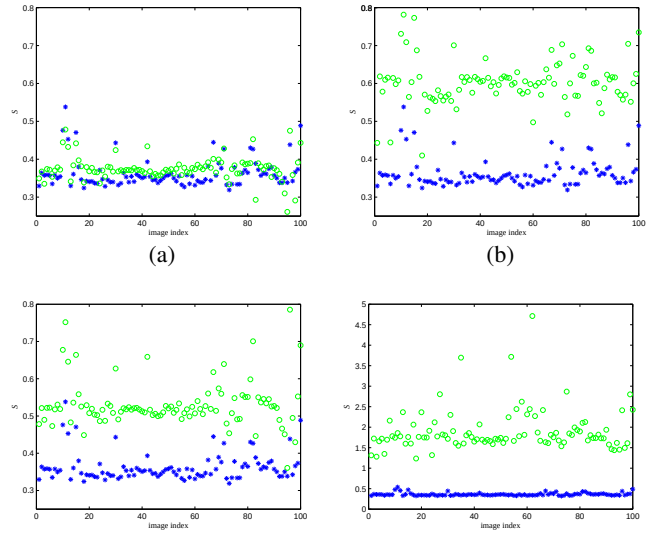

(a) (b) (c) (d)

Fig. 2. Scatter plots of S for original (blue asterisks) and enhanced (green circles) images. (a) Linear, $w = 0.6$ (separately), (b) linear, $w = 0.6$, (c) linear, $w = 1.2$, (d) Histogram equalization.

4. EXPERIMENTS

4.1. Experimental setup

To evaluate the performance of the proposed algorithm, 100 uncompressed color images sized 1600×1200 captured by commercial cameras are used in experiment. As in the previous work in [1, 3, 4], these images were enhanced by power law transformation (γ correction):

$$H(x) = [255(\frac{x}{255})^{\gamma}] \tag{12}$$

where $[\cdot]$ is a rounding operation. These enhanced image were combined with the unaltered images to create a testing database of 700 color images. Blocks of different sizes were segmented from the upper-left corner of these images. Each block was then classified as enhanced or unaltered by our proposed detection scheme using a variety of different thresholds to get a series of receiver operating characteristic (ROC) curves. Although we gained good results for different forms of contrast enhancements such as linear enhancement and histogram equalization, the results will be shown only for γ correction with γ randomly chosen from the set [0.5;0.8;1.2;1.5;1.8;2.0]. Notice that we did not enhance each color channel separately to avoid chromatic aberration. Instead, we converted RGB images into YUV color space and only applied contrast enhancement in Y channel as most contrast enhancement schemes do. Finally, the enhanced image will be converted back to RGB space. To provide a practical validation, we will show the detection results of a real cut-and-paste forgery.

4.2. Performance evaluation

The series of ROC curves for $c_1 = G$ and $c_2 = R$ in (11) are displayed in Fig. 3(a)-(d). P_D and P_{FA} marked in the figure denote the true positive rate and false positive rate, respectively. Results shown in Fig. 3 indicate that local contrast enhancement can be reliably detected even for testing blocks sized 16×16 pixels. With a P_{FA} of less than 5%, our method achieves a P_D of at least 90% using 16×16 pixels blocks for power law transformation and a P_D of around 95% achieved using 128×128 pixels blocks. One can see that the proposed method achieves better results than Stamm's algorithm with different cutoff frequencies T in case of small blocks sized 16×16 pixels and comparable performance for large blocks sized 128×128 pixels. Because for small blocks, the statistical significance of the calculated histogram would be reduced, so it is almost impossible to perform reliable contrast enhancement detection for small blocks sized below 50×50 pixels using histogram-based methods like [1]. It makes sense that larger blocks are more likely to contain sufficient high-frequency evidence, but the performance of the proposed algorithm decreases very little with the diminishing block sizes, implying the S extracted from small blocks, like 16×16 pixels, are competent to the classification task.

An example of a cut-and-paste image forgery is shown in Fig. 4(a)-(c), where a person is cut from Fig. 4(a), then transformed using the Photoshop Curve Tools and pasted on Fig. 4(b) to produce the composite image. To detect the forgery region, the image was segmented into 64×64 pixels blocks, and then our detection scheme was applied on each block for evidence of contrast enhancement. In Fig. 4(c), the blocks detected as contrast enhanced are highlighted in red square. Although the proposed algorithm fails on three all-white and two all-black blocks as they do not contain enough high-frequency content to provide high-frequency evidence, most of the enhanced blocks are reliably detected.

4.3. Performance under anti-forensics scenario

To investigate the performance of the proposed algorithm under anti-forensics scenario, two anti-forensics schemes proposed in [3] and [4] are used.

For method in [3], we added Gaussian noise $N(0, \sigma^2)$ in each channel of the contrast enhanced image. Detection results for image blocks sized 128×128 pixels are illustrated in Fig. 5(a)-(b). As expected, the proposed algorithm has good robustness against Gaussian noise. Because the additional noise can provide extra high-frequency evidence and therefore increase our confidence in the inter-channel similarities of high-frequency components, making it easy to detect contrast enhancement in case of additive noise.

Next, for the remapping scheme described in [4], it modifies the histogram h_y of an enhanced image according to the most similar histogram h_x from a reference histogram database by pixel remapping. It is worth mentioning that instead of applying remapping in enhanced Y channel, we remapped R, G and B channel of the final enhanced image for the reason that the conversion from YUV to RGB color space is essentially a per-pixel mapping, which will again introduce artifacts into histogram and neutralize the effect of anti-forensics algorithm. The comparison between the proposed method and Stamm's in [1] is given in Fig. 5(c)-(d). As we can see, remapped images can still be detected by Stamm's algorithm in case of large block sized 128×128 pixels, although the histograms of

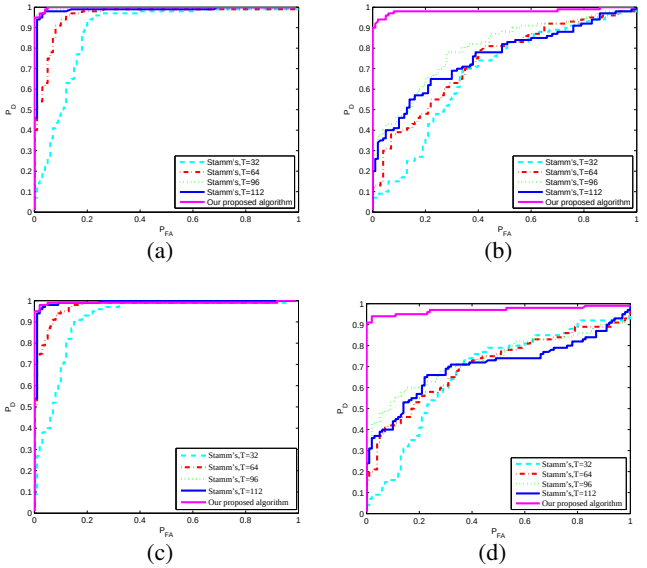

(a) (b) (c) (d)

Fig. 3. Detection ROC curves for images altered by γ correction. (a) $\gamma = 0.8$, blocksize=128×128, (b) $\gamma = 0.8$, blocksize=16×16, (c) $\gamma = 1.5$, blocksize=128×128, (d) $\gamma = 1.5$, blocksize=16×16.

(a) (b) (c)

Fig. 4. Cut-and-paste forgery detection example using 64×64 pixels blocks. (a) The untouched image from which an object is cut, (b) the untouched image into which the cut object is pasted, (c) the forged image.

produced anti-forensics images are smoother than those of enhanced images. But our algorithm still obtains better result. Actually, it achieves almost perfect result since the pixel remapping scheme is highly nonlinear, which will certainly disturb the inter-channel similarity as demonstrated in Section 3.2.

5. CONCLUSION

In this paper, we present a novel forensic method to expose cut-and-paste image forgery by detecting contrast enhancement in color images. Compared with the algorithm in [1], our proposed method is easier to implement and use, good results are still gained for small blocks sized 16×16 pixels. Besides, it has good robustness against some state-of-the-art anti-forensics schemes. However, both our proposed algorithm and that described in [1] are suffering from poor robustness against JPEG compression, so our future work will focus on improving robustness against image compression and combining with other detection methods.

6. ACKNOWLEDGEMENT

The authors would like to express sincere gratitude to M. Barni et al. for sharing the source code of algorithm in [4].

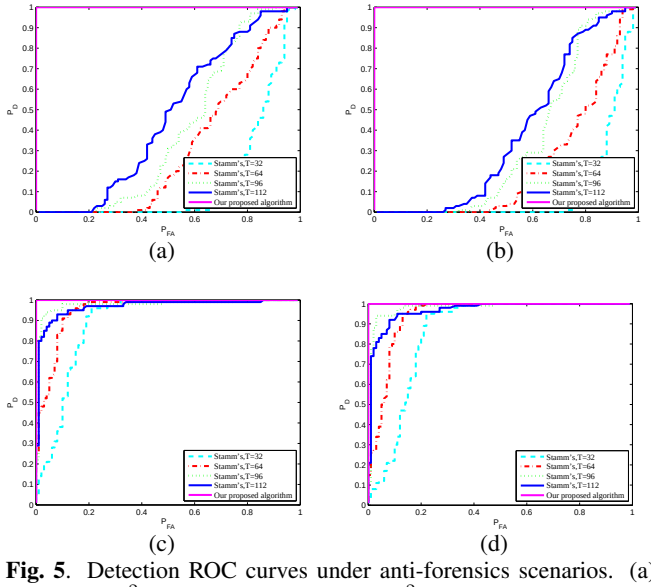

(a) (b) (c) (d)

Fig. 5. Detection ROC curves under anti-forensics scenarios. (a) $\gamma = 1.2$, $\sigma^2 = 0.01$, (b) $\gamma = 1.2$, $\sigma^2 = 0.05$, (c) $\gamma = 0.5$, blocksize=128×128, (d) $\gamma = 1.2$, blocksize=128×128.

7. REFERENCES

[1] M.C. Stamm and K.J.R. Liu, "Forensic detection of image manipulation using statistical intrinsic fingerprints," *IEEE Transactions on Information Forensics and Security*, vol. 5, no. 3, pp. 492–506, Sept. 2010.

[2] G.E. Healey and R. Kondepudy, "Radiometric ccd camera calibration and noise estimation," *IEEE Transactions on Pattern Analysis and Machine Intelligence*, vol. 16, no. 3, pp. 267–276, 1994.

[3] G. Cao, Y. Zhao, R. Ni, and H. Tian, "Anti-forensics of contrast enhancement in digital images," in *Proceedings of the 12th ACM Workshop on Multimedia and Security*, Roma, Italy, 2010, MM&Sec'10, pp. 25–34.

[4] M. Barni, M. Fontani, and B. Tondi, "A universal technique to hide traces of histogram-based image manipulations," in *Proceedings of the 14th ACM Workshop on Multimedia and Security*, Coventry, UK, 2012, MM&Sec'12, pp. 97–104.

[5] I. Pekkucuksen and Y. Altunbasak, "Edge strength filter based color filter array interpolation," *IEEE Transactions on Image Processing*, vol. 21, no. 1, pp. 393 –397, Jan. 2012.

[6] B.K. Gunturk, J. Glotzbach, Y. Altunbasak, R.W. Schafer, and R.M. Mersereau, "Demosaicking: color filter array interpolation," *IEEE Signal Processing Magazine*, vol. 22, no. 1, pp. 44–54, Jan. 2005.

[7] N.X. Lian, L. Chang, Y.P. Tan, and V. Zagorodnov, "Adaptive filtering for color filter array demosaicking," *IEEE Transactions on Image Processing*, vol. 16, no. 10, pp. 2515–2525, Oct. 2007.

[8] N.X. Lian, V. Zagorodnov, and Y.P. Tan, "Edge-preserving image denoising via optimal color space projection," *IEEE Transactions on Image Processing*, vol. 15, no. 9, pp. 2575–2587, Sept. 2006.

[9] C.L. Liu, "A tutorial of the wavelet transform," *NTUEE, Taiwan*, 2010.